Journal of Mathematics and Computer Science

A fish harvesting model with Allee effect and Holling type II functional response

Check for updates

Eihab B. M. Bashier

Faculty of Education and Arts, Sohar University, Sohar, Oman.

Faculty of Mathematical Sciences, University of Khartoum, Khartoum, Sudan.

Abstract

Fish harvesting is one of the most profitable investments as it does not require financial costs other than fishing equipment. Therefore, population harvesting models have become attractive to many researchers in the field of mathematical bio-economics. With so many models of fish harvesting, few of them discuss the use of Holling type II functional response to model the interaction between fish populations, harvest effort, and the conditions that are necessary to sustain fish harvesting in the long term. In this paper, we first present a differential equations model describing the dynamics of the fishes population under the presence of harvesting activity. We assume that, in the absence of harvesting activities, the growth dynamics of the fishes population is governed by a logistic growth with Allee effect. The harvesting term is represented by Holling type II functional response. The existence conditions for positive equilibrium point are derived, and the stability of the model equilibrium points are analyzed. An explicit fitted numerical method that is much faster than the Matlab's ODE solvers is developed to solve the model. Finally, numerical simulations are used to confirm the theoretical results.

Keywords: Fish harvesting, stability analysis, fitted numerical methods, Holling type II functional response, logistic growth with Allee effect.

2020 MSC: 34A34, 65L05.

1. Introduction

Fishing is one of eldest known to mankind, dating back to 40000 BC. In addition to fish being an important source of food, they are also profitable, and are used in the manufacture of many fish products used for non-food purposes. Currently, investing in fishing is one of the most profitable investments. The cost of fishing is limited to the equipment and human resources necessary to operate it, without incurring costs for fish production in the case of fishing from natural resources. After the industrial revolution, the means of fishing developed greatly, and the mechanisms of artificial fish production also developed.

Many mathematical models have been suggested in the literature to describe the dynamics of fish population under harvesting activity. In some fish harvesting models, the harvesting effort is described by a fixed or periodic harvesting terms [5, 6, 9, 12]. In many fish harvesting models, the interaction between fish population and effort excerted to catch them are looked at as prey-predator models. In

such a model the harvesting effort plays the role of predator, and the fish population plays the role of prey. Hence, in many of these models, the dynamics of fish population is described by either a logistic growth [1, 10], Gompertz growth [15] or logistic growth with Allee effect [8, 17], whereas the harvesting term is either assumed to be constant or described by type I functional response [18]. The dynamics of several discrete harvesting models of single species populations are discussed by [4]. The growth rates of such models included the logistic growth, logistic growth with Allee effect, and Ricker growth.

On the other hand, the term "functional response" was first used by Holling in 1959, to describe the predator intake rate to its food as a function of change in the density of available prey in a habitat [16]. Type I is a linear response in which the attack rate of the predator population individuals increases linearly with the density of the prey population and then suddenly reaches a constant value when the predators are satiated. In type II functional response, the predator population is assumed to spend its time in two types of activities: searching for prey and hunting of the prey (which includes stalking, killing, eating, and digesting). The rate of consumption in this model is limited because even assuming that the prey community is available and there is no need to spend time searching, predators still need to spend time in hunting. Type III has same assumptions as type II, but it further assumes that the rate of attacks of members of the predator population on members of the prey population accelerates at the beginning and slows down as it approaches the saturation level [7, 13].

Many models in the literature assume a type I functional response for the harvesting term, under the assumption that the harvesting effort is proportional to the fish intensity (see for example [12]). However, Idels [11] suggested other forms for the harvesting term.

In this paper we present a system of two ODEs representing the harvesting of fishes, where the dynamics of the fish population is represented by a logistic model with Alee effect, and the second equation describes the dynamics of the harvesting effort exerted to catch the fishes. We analyze the model for the existence and stability of positive steady state and present a numerical method for solving the model.

The rest of this paper is organized as follows. In Section 2, we present the model statement. Qualitative analysis of the model will be presented in Section 3. In Section 4, we present a numerical method for solving the model and illustrate the results of the numerical experiments. And finally, the discussions and conclusions will be presented in Section 5.

2. Model problem

In this section we present a system of two ODEs describing the dynamics of the fishes population and the effort exerted to catch them. The model compartments are: the abalone population denoted by $N(t)$ and the effort exerted in the fishes population, denoted by $E(t)$. The proposed model is given by the equations:

$$\dot{N}(t) = rN(t)\left(\frac{N(t)}{M} - 1\right)\left(1 - \frac{N(t)}{K}\right) - \frac{qN(t)E(t)}{\kappa + N(t)}, \quad N(0) = N_0 \; t \in [0, T], \tag{2.1}$$

$$\dot{E}(t) = \alpha\left(\frac{pqN(t)E(t)}{\kappa + N(t)} - cE(t)\right), \quad E(0) = E_0, \; t \in [0, T], \tag{2.2}$$

In this model, the growth rate of the fish population is represented by a logistic model with Alee effect. The parameter p is the average unit price and c is the per unit cost. The rate of change in effort is assumed to be proportional to the difference between the total profits and total expenses, where α is the proportionality constant.

The functional response term $\frac{qN(t)E(t)}{\kappa + N(t)}$ that appears in equations (2.1) and (2.2) is a second form of the type II functional response $\frac{aN(t)E(t)}{1 + a\theta N(t)}$, where a represents the catchability parameter and θ is the search rate (or rate of discovery). The parameters q and κ in model (2.1)-(2.2) are given by $q = 1/\theta$ and $\kappa = 1/(a\theta)$, respectively.

3. Qualitative analysis

The equilibria points of the model described by equations (2.1)-(2.2) are obtained by solving the system of linear equations:

$$rN(t)\left(\frac{N(t)}{M} - 1\right)\left(1 - \frac{N(t)}{K}\right) - \frac{qN(t)E(t)}{\kappa + N(t)} = 0, \tag{3.1}$$

$$\alpha\left(\frac{pqN(t)E(t)}{\kappa + N(t)} - cE(t)\right) = 0. \tag{3.2}$$

By solving Equation (3.2), we find that $E = 0$ or $N = \frac{c\kappa}{qp-c}$. Substituting $E(t) = 0$ in Equation (3.1) we obtain three equlibria points: $\text{Equi}(b_0) : (N_0^*, E_0^*) = (0, 0)$, $\text{Equi}(b_1) : (N_1^*, E_1^*) = (M, 0)$ and $\text{Equi}(b_2) : (N_2^*, E_2^*) = (K, 0)$. By substituting $N(t) = \frac{c\kappa}{qp-c} = \beta$ in Equation (3.1) we obtain the equilibria point:

$$\text{Equi}(b_3) : (N_3^*, E_3^*) = \left(\frac{c\kappa}{qp-c}, \frac{rp\beta(K-\beta)(\beta-M)}{cKM}\right), \quad \text{where } \beta = \frac{c \cdot \kappa}{qp - c}.$$

These four equilibrium points can be interpreted as follows.

(i) **The first equilibrium point** $\text{Equi}(b_0) = (0, 0)$**:** there are no fishes in the reserve and therefore no effort can be exerted to harvest them.

(ii) **The second equilibrium point** $\text{Equi}(b_1) = (M, 0)$**:** the fish population is at its minimum level, and any effort to harvest from it at this time will drop the fish stock below the threshold under which the fish population will extinct at the long term.

(iii) **The third equilibrium point** $\text{Equi}(b_2) = (K, 0)$**:** the fish population reaches its carrying capacity due to temporary prohibition (governmental or any stakeholders' policies) of fish harvesting at previous time to allow the fish population to grow. The level of fish population continues at this level until the policy is changed and harvesting from the population becomes allowed. For example, due to the high demand for abalone in the local and international markets, harvesting operations at the individual and corporate levels are intensively active during the abalone hunting seasons. Therefore, the Ministry of Agriculture and Water Resources in the Sultanate of Oman follows a policy of harvesting abalone for one year, and then banning fishing operations for a year or two to control the abalone stock in its areas of the coasts of the Dhofar Governorate and give it time to grow again, without reaching critical levels.

(iv) **The fourth equilibrium point** $\text{Equi}(b_3) = (\beta, rp\beta(K-\beta)(\beta-M)/(cKM))$**:** there is a safe level of fish in the reserve and the policies allow harvesting from the fish population.

The Jacobi matrix of system (2.1)-(2.2) is given by the form:

$$J(N, E) = \begin{bmatrix} \frac{-r(3N^2+KM-2KN-2MN)}{KM} - \frac{qE\kappa}{(\kappa+N)^2} & -\frac{qN}{\kappa+N} \\ \frac{\alpha pq\kappa E}{(\kappa+N)^2} & \alpha\left(\frac{qpN-c}{\kappa+N}\right) \end{bmatrix}. \tag{3.3}$$

To determine local stability of any equilibrium point $\text{Equi}(b_j, j) = 0, \dots, 3$, we evaluate the Jacobian matrix given by Equation (3.3) at such equilibrium and determine whether the real parts of its eigenvalues are both negative.

(i) **Local stability of** $\text{Equi}(b_0)$**:** The Jacobian matrix at $\text{Equi}(b_0) = (0, 0)$ is given by:

$$J_0^* = J(N_0^*, E_0^*) = \begin{bmatrix} -r & 0 \\ 0 & -\alpha c \end{bmatrix}.$$

Since J_0^* is a diagonal matrix, its eigenvalues are the diagonal elements. Hence, $\lambda_{0,1} = -r < 0$ and $\lambda_{0,2} = -\alpha c < 0$. Therefore, the equilibrium point $\text{Equi}(b_0)$ is locally asymptotically stable.

(ii) **Local stability of** $\text{Equi}(b_1) = (M, 0)$**:** The Jacobian matrix at $\text{Equi}(b_1) = (M, 0)$ is given by:

$$J_1^* = J(N_1^*, E_1^*) = \begin{bmatrix} r\left(1 - \frac{M}{K}\right) & -\frac{qM}{\kappa + M} \\ 0 & \alpha\left(\frac{pqM}{\kappa + M} - c\right) \end{bmatrix}.$$

Since J_1^* is upper triangular matrix, its eigenvalues are its diagonal elements. Hence, $\lambda_{1,1} = r\left(1 - \frac{M}{K}\right)$ > 0 (since $M < K$) and $\lambda_{1,2} = \alpha\left(\frac{pqM}{\kappa + M} - c\right)$. Therefore, the equilibrium point $\text{Equi}(b_1)$ is locally unstable.

(iii) **Local stability of** $\text{Equi}(b_2)$**:** The Jacobian matrix at $\text{Equi}(b_2) = (K, 0)$ is given by:

$$J_2^* = J(N_2^*, E_2^*) = \begin{bmatrix} r\left(1 - \frac{K}{M}\right) & -\frac{qK}{\kappa + K} \\ 0 & \alpha\left(\frac{pqK}{\kappa + K} - c\right) \end{bmatrix}.$$

Since J_2^* is upper triangular matrix, its eigenvalues are its diagonal elements. Hence, $\lambda_{2,1} = -r\left(\frac{K}{M} - 1\right)$ < 0 (since $K > M$) and $\lambda_{2,2} = \alpha\left(\frac{pqK}{\kappa + K} - c\right)$. Therefore, the equilibrium point $\text{Equi}(b_2)$ is locally asymptotically stable iff

$$\frac{pqK}{\kappa + K} < c, (\equiv \beta > K),$$

locally marginally stable iff

$$\frac{pqK}{\kappa + K} = c, (\equiv \beta = K),$$

and locally unstable iff

$$\frac{pqK}{\kappa + K} > c \;\; (\equiv \beta < K).$$

3.1. Positivity of E_3

We have $N_3^* = c \cdot \kappa / (qp - c)$ and we notice that both c and κ are positive, hence $c \cdot \kappa > 0$. If we suppose that $N_3^* > 0$, then that leads to $qp - c > 0$, which leads to the condition:

$$qp > c. \tag{3.4}$$

We suppose that Equation (3.4) holds. Then,

$$E_3^* > 0 \Rightarrow \frac{rp\beta(K - \beta)(\beta - M)}{qKM} > 0.$$

Since the denominator $cKM > 0$, then $rp\beta(K - \beta)(\beta - M) > 0$, which implies that

$$(K - \beta)(\beta - M) > 0.$$

It is either both $K - \beta > 0$ and $\beta - M > 0$ which means $M < \beta < K$, or $K - \beta < 0$ and $\beta - M < 0$, which means $K < \beta < M$. This later is rejected since given $K > M$.

By writing $c \cdot \kappa / (qp - c)$ instead of β, we have:

$$M < \frac{c \cdot \kappa}{qp - c} < K,$$

which leads to the second condition:

$$\frac{qpM}{\kappa + M} < c < \frac{qpK}{\kappa + K}. \tag{3.5}$$

Hence, the positivity conditions of E_3 can be stated through the following theorem.

Theorem 3.1. *The equilibrium point* $(N_3^*, E_3^*) = \left(\beta, \frac{rp\beta(K-\beta)(\beta-M)}{cKM}\right)$ *is positive, if the following two conditions hold:*

  (i) $qp - c > 0$; *and*
  (ii) $\frac{qpM}{\kappa+M} < c < \frac{qpK}{\kappa+K}$.

3.2. Local stability of E_3

Equations (3.4) and (3.5) indicate that the existence of a positive equilibrium $\text{Equi}(b_3)$ depends on the value of β, where β must lie in (M, K) $(M < \beta < K)$. If either $\beta < M$ or $\beta > K$ the system will have only three equilibria points. This is telling us to study the effects of the parameters in β (p, q and c) to the dynamic of the system. Hence, we consider particularly parameters c and κ.

To study the stability of E_3, first we evaluate the Jacobi matrix $J(N, E)$ at (N_3^*, E_3^*) to obtain:

$$J_3^* = J(N_3^*, E_3^*) = \begin{bmatrix} \frac{-cr[(\kappa+K)(\kappa+M)c^2+2pq(\kappa^2-KM)c+p^2q^2(KM-\kappa(K+M))]}{pqKM(pq-c)^2} & -\frac{c}{p} \\ \frac{-\alpha r(\kappa c-K(pq-c))(\kappa c-M(pq-c))}{qKM(pq-c)} & 0 \end{bmatrix}.$$

The characteristic equation of J_3^* is given by:

$$\lambda^2 + \sigma\lambda + \delta = 0,$$

where

$$\sigma = -\text{trace}(J_3^*) = \frac{cr\left[\frac{c^2\kappa^2}{(pq-c)^2} - \frac{K\kappa(p^2q^2)}{(pq-c)^2} - \frac{M\kappa(p^2q^2-c^2)}{(pq-c)^2} + \frac{KM(pq-c)^2}{(pq-c)^2} + \frac{2pqc^2\kappa^2}{(pq-c)^2}\right]}{pqKM}$$

$$= \frac{cr\left[\beta^2 + \frac{K+M}{2}(pq+c)\beta + KM + \frac{2pq}{c}\beta^2\right]}{pqKM}$$

$$= \frac{r\left[(2pq+c)\beta^2 - (K+M)(pq+c)\beta + cKM\right]}{pqKM}$$

and

$$\delta = \det(J_3^*) = \frac{-\alpha cr(\kappa c - K(pq-c))(\kappa c - M(pq-c))}{pqKM(pq-c)}$$

$$= \frac{-\alpha cr(\kappa c - K(pq-c))\left(\frac{\kappa c}{pq-c} - M\right)}{pqKM}$$

$$= \frac{\alpha cr(pq-c)\left(K - \frac{\kappa c}{pq-c}\right)\left(\frac{\kappa c}{pq-c} - M\right)}{pqKM}$$

$$= \frac{\alpha cr(pq-c)(K-\beta)(\beta-M)}{pqKM}.$$

From its characteristic equation, the eigenvalues of J_3^* are given by:

$$\lambda_{3,1} = \frac{-\sigma + \sqrt{\sigma^2 - 4\delta}}{2}, \qquad\qquad \lambda_{3,2} = \frac{-\sigma - \sqrt{\sigma^2 - 4\delta}}{2}.$$

The discriminant $D^2 = \sigma^2 - 4\delta$ determines whether the eigenvalues of J_3^* are real or complex (depending on whether the discriminant is non-negative or negative, respectively). The equilibrium point $\text{Equi}(b_3)$ is asymptotically stable if the real parts of its eigenvalues are negative. This can be achieved if and only if $\sigma > 0$ and $\delta > 0$ in both the cases $D^2 \geqslant 0$ (real eigenvalues) or $D^2 < 0$ (complex eigenvalues) [14].

We assume that the conditions $pq - c > 0$ and $M \leqslant \beta \leqslant K$ (described by equations (3.4) and (3.5), which guarantee that Equi(b_3) is non-negative) are fulfilled and therefore δ is always positive. Hence, to determine the stability of Equi(b_3), we will discuss different scenarios about $\sigma = -\text{trace}(J_3^*)$.

The solutions of $\delta = 0$ in parameter c are given by

$$c_{\delta_0} = 0, \qquad\qquad c_{\delta_1} = \frac{pqM}{\kappa + M}, \qquad\qquad c_{\delta_2} = \frac{pqK}{\kappa + K}.$$

The assumption that $\delta > 0$, which requires that $\beta > M$ implies that $c > \frac{pqM}{\kappa+M}$. Hence, for $0 \leqslant c \leqslant c_{\delta_1}$, the equilibrium point Equi(b_2) is unstable as stated in Theorem 3.1 and the only stable node is Equi(b_0). Therefore, hereafter we assume that $c_{\delta_1} < c < c_{\delta_2}$. Since δ has three roots $(0, c_{\delta_1} \& c_{\delta_2})$, it does not change its sign within either of the intervals $(0, c_{\delta_1}), (c_{\delta_1}, c_{\delta_2})$, or (c_{δ_2}, ∞). That means δ is either positive or negative in $(c_{\delta_1}, c_{\delta_2})$.

Assume that $\frac{pqM}{\kappa+M} < c < \frac{pqK}{\kappa+K}$ and $pq > c$. Let $\epsilon > 0$ be a small positive real number. Then,

$$\delta(c_{\delta_1} + \epsilon) = \frac{\alpha r \epsilon \left(p^2 q^2 \kappa M(K-M) + pq(\kappa+M)\left(K(\kappa-M) - 2KM\right)\epsilon - (\kappa+M)^2(\kappa+K)\epsilon^2 \right)}{pqKM(pq-c)}.$$

Since the coefficient of ϵ is given by $p^2q^2\kappa M(K-M) > 0$, then $\delta > 0$ in $(c_{\delta_1}, c_{\delta_2})$ for all $\kappa > 0$.

To determine where σ changes its sign, we have

$$\sigma = \frac{cr\left[(\kappa+K)(\kappa+M)c^2 + 2pq(\kappa^2 - KM)c + p^2q^2(KM - \kappa(K-M))\right]}{pqKM(pq-c)^2}.$$

Now,

$$\sigma = 0 \Rightarrow \frac{cr\left[(\kappa+K)(\kappa+M)c^2 + 2pq(\kappa^2 - KM)c + p^2q^2(KM - \kappa(K+M))\right]}{pqKM(pq-c)^2} = 0$$

$$\Rightarrow cr\left[(\kappa+K)(\kappa+M)c^2 + 2pq(\kappa^2 - KM)c + p^2q^2(KM - \kappa(K+M))\right] = 0$$

$$\Rightarrow c = c_1 = 0, \quad \text{or } (\kappa+K)(\kappa+M)c^2 + 2pq(\kappa^2 - KM)c + p^2q^2(KM - \kappa(K+M)) = 0.$$

A positive solution of the quadratic equation:

$$(\kappa+K)(\kappa+M)c^2 + 2pq(\kappa^2 - KM)c + p^2q^2(KM - \kappa(K+M)) = 0, \tag{3.6}$$

such that $\sigma = 0$, can always be found. This can be shown as follows:

(i) In the case $\kappa < (KM)/(K+M)(< M)$, we notice that $KM - \kappa(K+M) > 0$ and $\kappa^2 = \kappa \cdot \kappa < KM$. Hence, $p^2q^2(KM - \kappa(K+M)) > 0$ and $2pq(\kappa^2 - KM) < 0$. This guarantees that Equation (3.6) has two positive roots.

(ii) In the case $\kappa > (KM)/(K+M)$ the term $KM - \kappa(K+M)$ is always negative, hence Equation (3.6) has one positive root and one negative root.

The solutions of Equation (3.6) are given by:

$$c_{\sigma_1} = \frac{pq\left(KM - \kappa^2 - \kappa\sqrt{K^2 + K\kappa - KM + \kappa^2 + \kappa M + M^2}\right)}{(\kappa+M)(\kappa+K)}$$

and

$$c_{\sigma_2} = \frac{pq\left(KM - \kappa^2 + \kappa\sqrt{K^2 + K\kappa - KM + \kappa^2 + \kappa M + M^2}\right)}{(\kappa+M)(\kappa+K)}.$$

We notice that either $c_{\sigma_1} < 0$, $c_{\sigma_0} = 0$ and $c_\sigma^* > 0$ in case of $\kappa > (KM)/(K+M)$ or $c_{\sigma_0} = 0, c_{\sigma_2} > 0$ and $c_{\sigma_1} > 0$ if $\kappa \leqslant (KM)/(K+M)$.

In the case that $\kappa < (KM)/(K+M)$, we have $c_{\delta_0} = c_{\sigma_0} = 0 < c_{\sigma_1} < c_{\delta_1} < c_{\sigma_2} < c_{\delta_2}$. In the case that $\kappa > M$, we have $c_{\sigma_1} < 0 < c_{\delta_1} < c_{\sigma_2} < c_{\delta_2}$.

In the interval $[0, c_{\delta_1}]$, we have $\delta < 0$ and the only stable node is Equi(b_0) given by $(0,0)$. Hence, we restrict our focus on the interval $(c_{\delta_1}, c_{\delta_2})$ which always includes the point $c = c_{\sigma_2}$. We wish to determine the sign of σ in both the intervals $(c_{\delta_1}, c_{\sigma_2})$ and $(c_{\sigma_2}, c_{\delta_2})$.

Since σ does not change its sign within either of the intervals $(0, c_{\sigma_1})$, $(c_{\sigma_1}, c_{\sigma_2})$, and (c_{σ_2}, ∞), and the quantities r and $pqKM(pq - c)^2$ are positive, the sign of sigma in $(c_{\delta_1}, c_{\delta_2})$ is determined by the sign of

$$\varphi_\sigma(c) = c \left((\kappa + K)(\kappa + M)c^2 + 2pq(\kappa^2 - KM)c + p^2q^2(KM - \kappa(K + M)) \right).$$

The function φ_σ satisfies $\varphi_\sigma(0) = \varphi_\sigma(c_{\sigma_1}) = \varphi_\sigma(c_{\sigma_2}) = 0$. Therefore, the function φ_σ does not change its sign in either of the intervals $(0, c_{\sigma_1})$, $(c_{\sigma_1}, c_{\sigma_2})$, or (c_{σ_2}, ∞). To determine the signs of $\varphi_\sigma(c)$ for $c \in (c_{\delta_1}, c_{\sigma_2})$, and $(c_{\sigma_2}, c_{\delta_2})$, let ϵ an arbitrary small positive real number. Then,

$$\varphi_\sigma(c_{\sigma_2} - \epsilon) = -\left(2pq(\kappa^2 - KM) + 2 * (\kappa + K)(\kappa + M) * c_{\sigma_2} \right) \epsilon + \mathcal{O}(\epsilon^2), \tag{3.7}$$

which shows that $\sigma < 0$ in $(c_{\delta_1}, c_{\sigma_2})$. On the other hand,

$$\varphi(c\sigma_2 + \epsilon) = \varphi_\sigma(c_{\sigma_2} + \epsilon) = \left(2pq(\kappa^2 - KM) + 2 * (\kappa + K)(\kappa + M) * c_{\sigma_2} \right) \epsilon + \mathcal{O}(\epsilon^2), \tag{3.8}$$

which shows that $\sigma > 0$ in (c_{σ_2}, ∞). Let

$$c_\sigma^* = c_{\sigma_2} = \frac{pq \left(KM - \kappa^2 + \kappa\sqrt{K^2 + K\kappa - KM + \kappa^2 + \kappa M + M^2} \right)}{(\kappa + M)(\kappa + K)}. \tag{3.9}$$

Equations (3.7) and (3.8) indicate that $c = c_\sigma^*$ is the value at which σ changes its sign from negative to positive, causing changes in the signs of the real parts of the eigenvalues $\lambda_{3,1}$ and $\lambda_{3,2}$ from positive to negative. That means J_3^* changes its stability status from unstable to a stable equilibrium, when c crosses from values less than c_σ^*, through c_σ^* to values greater than c_σ^*.

Based on equations (3.5), (3.7), (3.8), and (3.9), we have the following theorem.

Theorem 3.2. *In the system* (2.1)-(2.2), *if* $pq > c$ *and* $M < \beta < K$, *then the equilibrium point* Equi(b_3) $=$ $(\beta, rp\beta(K - \beta)(\beta - M)/(cKM))$ *is asymptotically stable iff*

$$c_\sigma^* < c < \frac{pqK}{\kappa + K},$$

and unstable if $0 \leqslant c \leqslant c_\sigma^*$ *or* $c \geqslant \frac{pqK}{\kappa + K}$.

To find the points at which the eigenvalues change from real to complex or vice versa, we have to solve the equation $\sigma^2 - 4\delta = 0$. We have

$$\sigma^2 - 4\delta = \frac{cr \left(A_5 c^5 + A_4 c^4 + A_3 c^3 + A_2 c^2 + A_1 c + A_0 \right)}{K^2 M^2 p^2 q^2 (pq - c)^4},$$

where,

$A_5 = r (K + \kappa)(\kappa + M)(r(K + \kappa)(\kappa + M) - 4\alpha pqKM)$,

$A_4 = 4rpq \left[r \left(\kappa^4 - K^2M^2 + K\kappa^3 + \kappa^3M - K\kappa M^2 - K^2\kappa M \right) + \alpha pqKM \left(5KM + 4\kappa M + 3\kappa^2 + 4K\kappa \right) \right]$,

$A_3 = -2rp^2q^2[r(\kappa^2(K(K + \kappa + 5M) + \kappa(M - 2\kappa) + M^2) - 3K^2M^2) + 2\alpha pqKM(2M(5K + 3\kappa) + 3\kappa(\kappa + 2K))]$,

$A_2 = 4rp^3q^3 \left[r \left(K(M(\kappa M - KM + \kappa^2 + K\kappa) - \kappa^3) - \kappa^3M \right) + \alpha pqKM \left(10KM + 4\kappa M + \kappa^2 + 4K\kappa \right) \right]$,

$A_1 = rp^4q^4 \left[r(K^2\kappa^2 + K^2M^2 + \kappa^2M^2 - 2K\kappa M^2 + 2K\kappa^2M - 2K^2\kappa M) - 4\alpha pqKM(5KM - \kappa M - K\kappa) \right]$,

$A_0 = 4r\alpha p^6 q^6 K^2 M^2$.

Now,

$$\sigma^2 - 4\delta = 0 \Rightarrow c_1 = 0 \text{ or } A_5 c^5 + A_4 c^4 + A_3 c^3 + A_2 c^2 + A_1 c + A_0 = 0.$$

Let $P(c) = A_5 c^5 + A_4 c^4 + A_3 c^3 + A_2 c^2 + A_1 c + A_0$. It is very hard to compute the roots of the fifth degree polynomial $P(c)$ for the set of general parameters, even by using computer algebra systems. But, we have the following notices about $P(c)$.

(i) A_0 is always positive.

(ii) The sign of the leading coefficient A_5 depends on the sign of $r(K + \kappa)(\kappa + M) - 4\alpha pqKM = r\kappa(K + \kappa + M) + (r - \alpha pq)KM$. If the parameters α, p, q, and r lie in the same scale, then it is more likely that A_5 is positive.

(iii) If $\kappa^2 > KM$, then A_4 will be positive because $\kappa^4 > K^2M^2$, $K\kappa^3 > K^2\kappa M$, and $\kappa^3 > K\kappa M^2$, while the remaining terms are positive.

(iv) A_3 is more likely to be negative, since most of the terms it contains are negative with few positive terms.

(v) After collecting terms, A_2 consists of two terms. The second term $\alpha pqKM(10KM + 4\kappa M + \kappa^2 + 4K\kappa)$ is always positive. There is no more likely possibility as to whether the sign of the first term is positive or negative. But considering both terms, we think that the sign of A_2 is more likely to be positive.

Considering the above notices about the coefficients of $P(c)$, and using the Descartes rule of signs, we can expect that there are at most two positive roots of $P(c)$ if $A_1 > 0$ and at most four positive roots if $A_1 < 0$. However, through many numerical experiments, we found that there are always two positive roots of $P(c)$, which we will refer to as c_1^* and c_2^* such that $0 < c_1^* < c_\sigma^* < c_2^* < pqK/(\kappa + K)$. According to these values ($\{0, c_1^*, c_\sigma^*, c_2^*, pqK/(\kappa + K)\}$), the c-space is divided into regions such that

(I) for $0 < c < c_1^*$, the eigenvalues $\lambda_{3,1}$ and $\lambda_{3,2}$ are real and positive, hence, the equilibrium point Equi(b_3) is unstable;

(II) for $c_1^* < c < c_\sigma^*$, the eigenvalues $\lambda_{3,1}$ and $\lambda_{3,2}$ are complex with positive real parts, hence, the equilibrium point Equi(b_3) is unstable;

(III) if $c_\sigma^* < c < c_2^*$, the eigenvalues $\lambda_{3,1}$ and $\lambda_{3,2}$ are complex with negative real parts, hence, the equilibrium point Equi(b_3) is stable;

(IV) for $c_2^* < c < pqK/(K + \sigma)$, the eigenvalues $\lambda_{3,1}$ and $\lambda_{3,2}$ are real and negative, hence, the equilibrium point Equi(b_3) is stable. This show that a transcritical bifurcation occurs at the point $c = c_2^*$.

An important notice here is that the signs of the real parts of the complex eigenvalues $\lambda_{3,1}$ and $\lambda_{3,2}$ are changed from positive to negative when c crosses from the interval (c_1^*, c_σ^*) through c_σ^* to $(c_\sigma^*, pqK/(\kappa + K))$, showing that a Hopf bifurcation occurs at $c = c_\sigma^*$.

According to the above mentioned properties of the eigenvalues of J_0^*, J_1^*, J_2^* and J_3^*, the stability of the equilibrium points Equi(b_0), Equi(b_1), Equi(b_2), and Equi(b_3) are summarized as follows.

(i) If $0 < c \leqslant c_\sigma^*$, then Equi($b_0$) is the only stable equilibrium point. Hence, for any initial starting point $N_\infty \to N_0^* = 0$ and $E_\infty \to E_0^* = 0$.

(ii) If $c_\sigma^* < c < \frac{pqK}{\kappa+K}$, then both Equi($b_0$) and Equi($b_3$) are stable. Hence, any starting initial condition ends at either $N_\infty \to N_0^* = 0, E_\infty \to E_0^* = 0$ or $N_\infty \to N_3^* = \beta, E_\infty \to E_3^* = p\beta(\beta - M)(K - \beta)/(cKM)$.

(iii) If $c > pqK/(\kappa + K)$, then both Equi(b_0) and Equi(b_2) are stable. Hence, any starting initial condition ends at $N_\infty \to N_0^* = 0, E_\infty \to E_0^* = 0$ or $N_\infty \to N_2^* = K, E_\infty \to E_2^* = 0$.

(iv) The equilibrium point Equi(b_1) is always unstable. Hence, any starting initial point that is close to Equi(b_1) ends either at either Equi(b_0), Equi(b_2) or Equi(b_3).

4. Numerical results

We propose a positivity preserving fitted numerical method as in [2, 3] for solving the system (2.1)-(2.2) in $[0, T]$. The time space $[0, T]$ is divided into n subintervals of equal lengths h, where $h = T/n$. The concepts of denominator functions and nonlocal approximations are used to design the following explicit finite difference formulas:

$$\frac{N_{j+1} - N_j}{\phi_1} = -rN_{j+1} + \frac{r(K + M)}{KM}N_j^2 - \frac{rN_j^2}{KM}N_{j+1} - \frac{qN_{j+1}E_j}{\kappa + N_j}, N(0) = N_0, \ j = 0, \ldots, n-1, \tag{4.1}$$

$$\frac{E_{j+1} - E_j}{\phi_2} = \frac{\alpha p q N_j E_j}{\kappa + N_j} - c E_{j+1}, \quad E(0) = E_0, \quad j = 0, \dots, n-1, \tag{4.2}$$

where the denominator function ϕ_1 and ϕ_2 are given by the forms $\phi_1 = \frac{1 - e^{-rh}}{r}$ and $\phi_2 = \frac{1 - e^{-\alpha ch}}{\alpha c}$. The numerical scheme (4.1)-(4.2) can be simplified into

$$N_{j+1} = \frac{\left(1 + r\phi_1(h)\left(\frac{1}{K} + \frac{1}{M}\right)N_j\right)N_j}{1 + \phi_1\left(r + \frac{rN_j^2}{KM} + \frac{qE_j}{\kappa + N_j}\right)}, \quad N(0) = N_0, \quad j = 0, \dots, n-1, \tag{4.3}$$

$$E_{j+1} = \frac{(1 + \alpha\phi_2(h)pqN_j)E_j}{(\kappa + N_j)(1 + \alpha c\phi_2)}, \quad E(0) = E_0, \quad j = 0, \dots, n-1. \tag{4.4}$$

We notice that the numerical scheme (4.3)-(4.4) is explicit, and whenever $N_0 > 0$ & $E_0 > 0$, then $N_j > 0 \ \forall j \geqslant 0$ and $E_j > 0 \ \forall j \geqslant 0$. That is (4.3)-(4.4) preserves the positivity of the solution for any positive initial conditions.

Now, we provide numerical simulations confirming the stability analysis results obtained in Section 3. The values of the model parameters are taken as follows. $M = 10, K = 100, \kappa = 60, q = 0.6, p = 0.2$ and $\alpha = 1.0$. We consider two values for the parameter r, the first is $r = 0.2$, which is close to $\alpha pq = 0.12$, and the second is $r = 0.02$, which is much less than αpq. When $r = 0.2$ we set $N(0) = 70, E(0) = 40$ and $T = 3000$, and when $r = 0.02$ we set $N(0) = 90, E(0) = 10$ and $T = 4000$.

To show that for any $\kappa > 0$, there exists c_σ^*, such that the equilibrium point E_3^* is unstable for $c < c_\sigma^*$ and stable for $c > c_\sigma^*$, we considered values of κ such that $0 < \kappa < 2K$ and against any value of κ we plotted the values $pqM/(\kappa + M)$, c_σ^* and $pqK/(\kappa + K)$. Figures 1a and 1b show the values of $c_{\delta_1}, c_\sigma^*, c_2^*$, and c_{δ_2} against the values of κ where $0 < \kappa < 2K$.

(a) $r = 0.2$

(b) $r = 0.02$
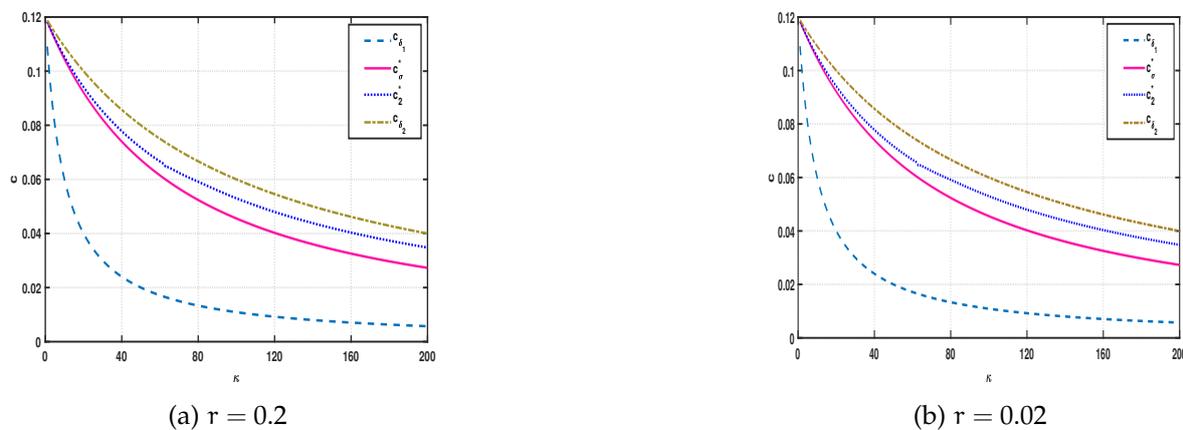
Figure 1: The values of $c_{\delta_1}, c_\sigma^*, c_2^*$, and $c_{\delta_2}^*$ against values of κ for $0 < \kappa < 2K$.

With these set of parameters and when $r = 0.2$, we have $c_1^* \approx 0.056646840$, $c_\sigma^* \approx 0.0614514256$, $c_2^* \approx 0.0643994831$, $pqK/(\kappa + K) = 0.075$, $N_3^* = 62.8668942$, and $E_3^* = 80.4004905$. When $r = 0.02$, we have $c_1^* \approx 0.024128186$, $c_\sigma^* \approx 0.0614514256$, $c_2^* \approx 0.068137799$, $pqK/(\kappa + K) = 0.075$, $N_3^* = 62.8668942$, and $E_3^* = 8.04004905$ (no change in c_σ^* and $pqK/(\kappa + K)$ as they do not depend on r).

To show that Hopf bifurcations occur at $c_\sigma^* \approx 0.0614514256$ when $r = 0.2$ or $r = 0.02$, we developed Matlab codes to plot the bifurcation diagrams in either of the two cases, where 500 values of parameter c in the interval $[0.06, 0.063]$ with 200 random initial conditions in the interval $N_0 \in (89, 91)$, $E_0 = 5$ are used to compute N_∞ and E_∞. Figure 2 shows the bifurcation diagram in the case $r = 0.2$.

For $r = 0.2$ we consider six values of the parameter c, which are $0.0612, 0.0614, 0.0615, 0.0616, 0.07$, and 0.08. For $r = 0.02$ we consider the values $0.0610, 0.0614, 0.0615, 0.0617, 0.07$, and 0.08 of parameter c.
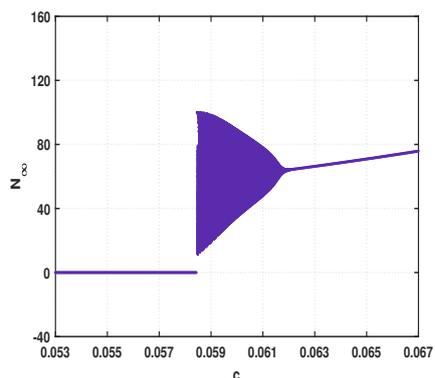
Figures 3, 4, 5, and 6 illustrate the dynamics of the fishes population and harvesting effort obtained by the numerical simulations for selected values of parameter c below and above the critical value c_σ^*.
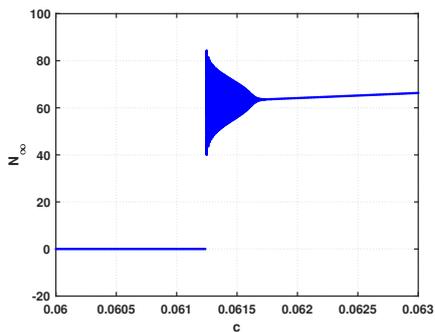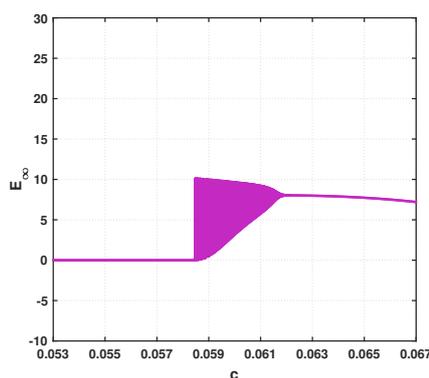
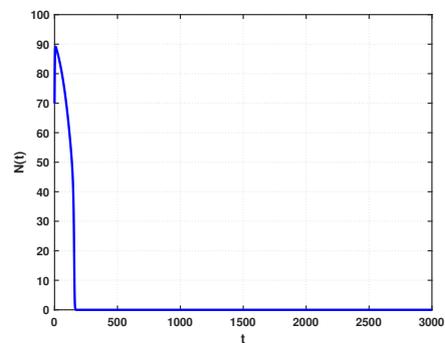(a) Fishes population.
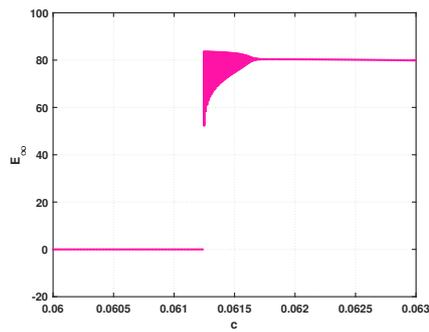
(b) Harvesting effort.
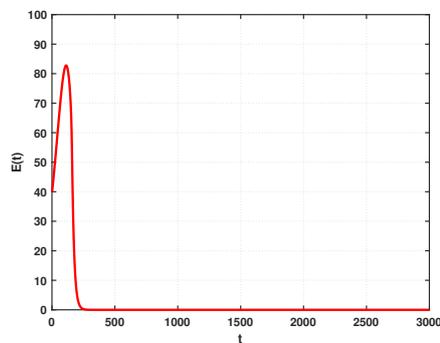

(c) Fishes population.
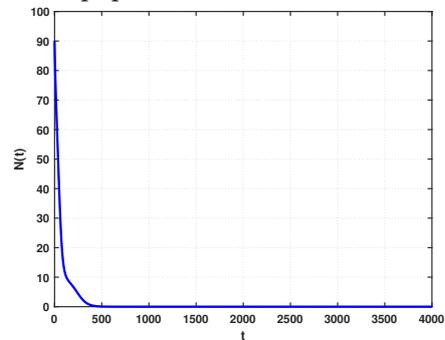

(d) Harvesting effort.

Figure 2: Bifurcation diagrams for the fishes population and harvesting effort, with $c \in [0.06, 0.063]$ and $r = 0.2$ (Figures 2a and 2b) and $c \in [0.054, 0.066]$ and $r = 0.02$ (Figures 2c and 2d).
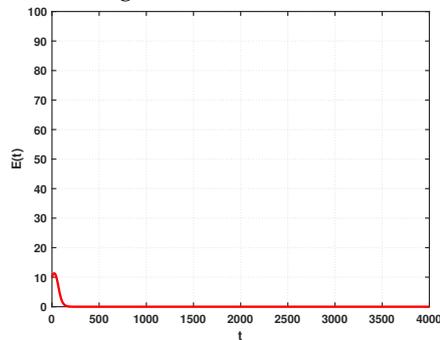

(a) Fishes population: $r = 0.2$ and $c = 0.0612$.
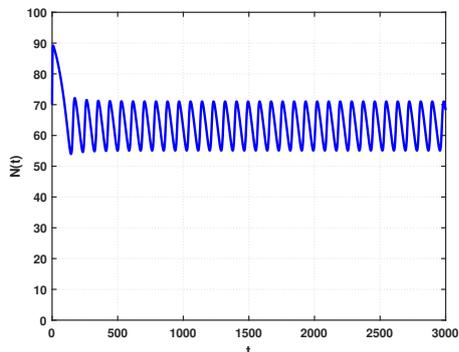

(b) Harvesting effort: $r = 0.2$ and $c = 0.0612$.
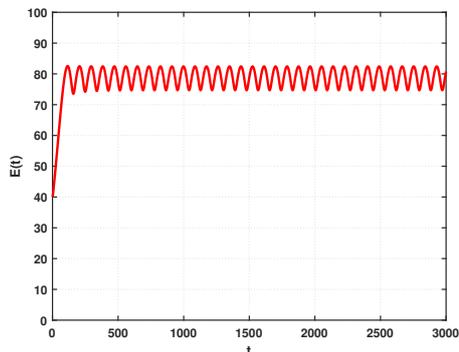

(c) Fishes population: $r = 0.02$ and $c = 0.0610$.

(d) Harvesting effort: $r = 0.02$ and $c = 0.061$.

Figure 3: Fishes populations vs harvesting efforts for $r = 0.2, c = 0.0612$ and $r = 0.02, c = 0.061$.

In Figures 3a,3b, 3c, and 3d the parameter c is set to the value 0.0612 which is below c_σ^*. Hence, both the dynamics of fishes population and harvesting effort tend to $\text{Equi}(b_0) = (0,0)$ at the long run.

(a) Fishes population percentage $c = 0.0614$.
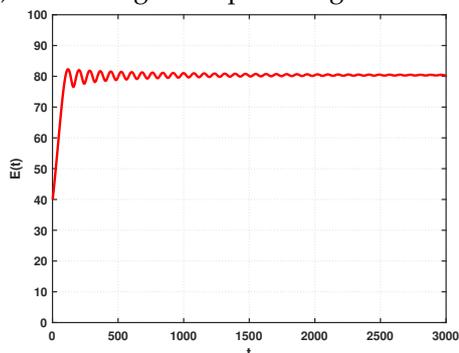

(b) Harvesting effort percentage $c = 0.0614$.
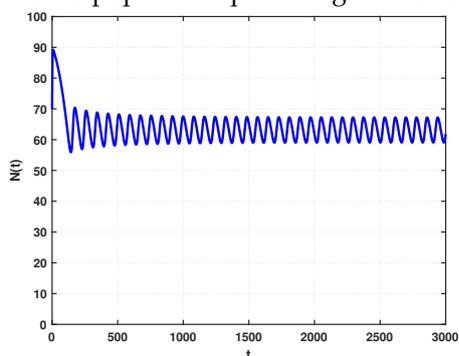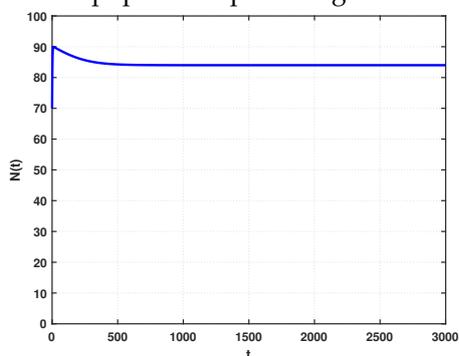

(c) Fishes population percentage $c = 0.0615$.
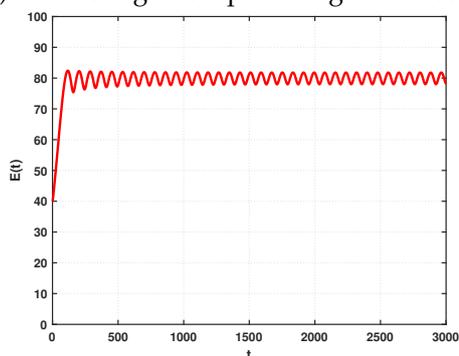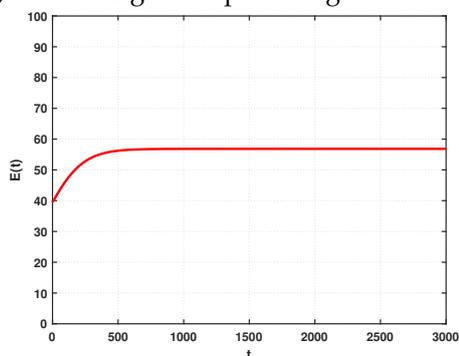

(d) Harvesting effort percentage $c = 0.0615$.
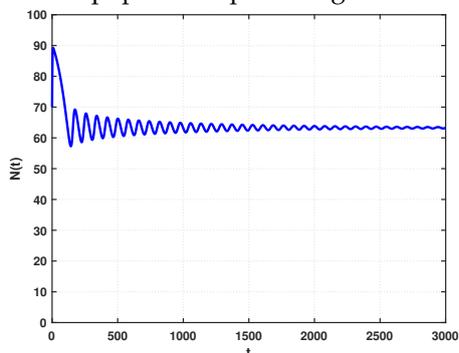
(e) Fishes population percentage $c = 0.0616$.
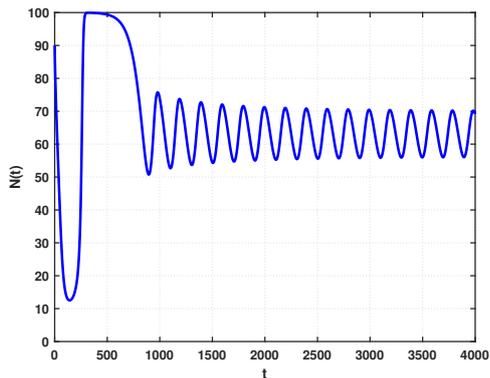

(f) Harvesting effort percentage $c = 0.0616$.
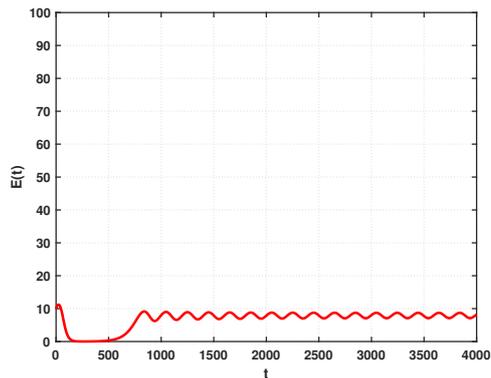

(g) Fishes population percentage $c = 0.0700$.

(h) Harvesting effort percentage $c = 0.0700$.
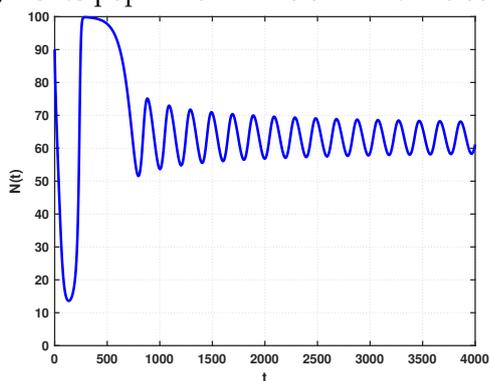
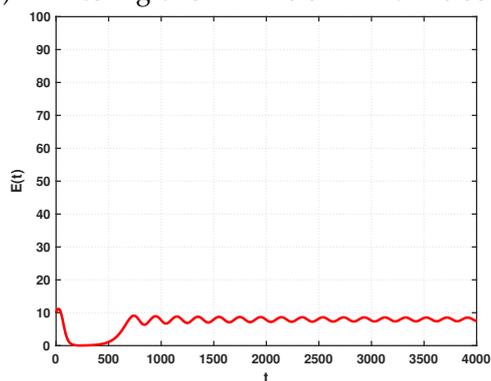Figure 4: Fishes population vs harvesting effort for $r = 0.2$ and different values of c.
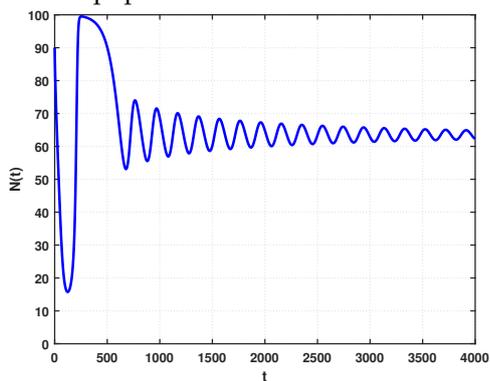
(a) Fishes population: $r = 0.02$ and $c = 0.0614$.
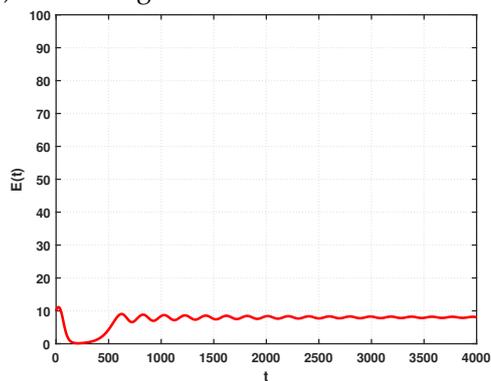
(b) Harvesting effort: $r = 0.02$ and $c = 0.0614$.

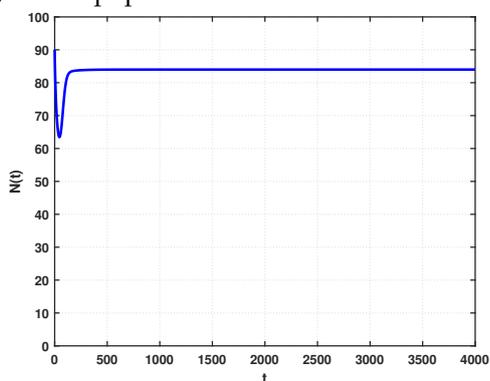(c) Fishes population: $r = 0.02$ and $c = 0.0615$.
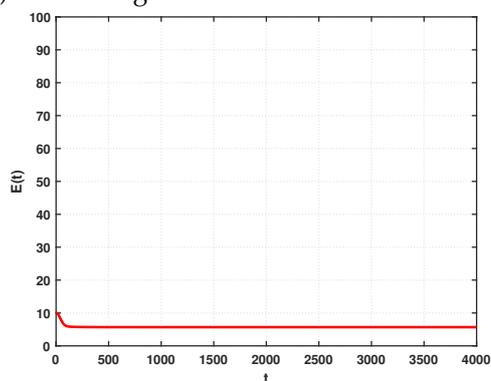
(d) Harvesting effort: $r = 0.02$ and $c = 0.0615$.

(e) Fishes population: $r = 0.02$ and $c = 0.0617$.

(f) Harvesting effort: $r = 0.02$ and $c = 0.0617$.

(g) Fishes population: $r = 0.02$ and $c = 0.0700$.

(h) Harvesting effort: $r = 0.02$ and $c = 0.0700$.

Figure 5: Fishes population vs harvesting effort for $r = 0.02$ and different values of c.

When $c = 0.0614$, which is too close the critical value c_σ^*, we see from Figures 4a, 4b, 5a, and 5b that the fishes population and harvesting effort oscillate around the equilibrium point Equi(b_3). As c passes c_σ^* to the value 0.0615 (which is less than c_2^*), the long term dynamics of the fishes population and harvesting effort converges the equilibrium point Equi(b_3) as can be seen in Figures 4c, 4d, 5c, 5d, and also in Figures 4e, 4f, 5e, and 5f. When $c = 0.07 > c_2^*$, the dynamics of the fishes population and harvesting effort converge to the equilibrium point Equi(b_3) without oscillations as appears in Figures 4g, 4h, 5g, and 5h. This is due to the fact that the eigenvalues of J_3^* are real negative.

(a) Fishes population: $r = 0.2$ and $c = 0.08$.

(b) Harvesting effort: $r = 0.2$ and $c = 0.08$.

(c) Fishes population: $r = 0.02$ and $c = 0.08$.
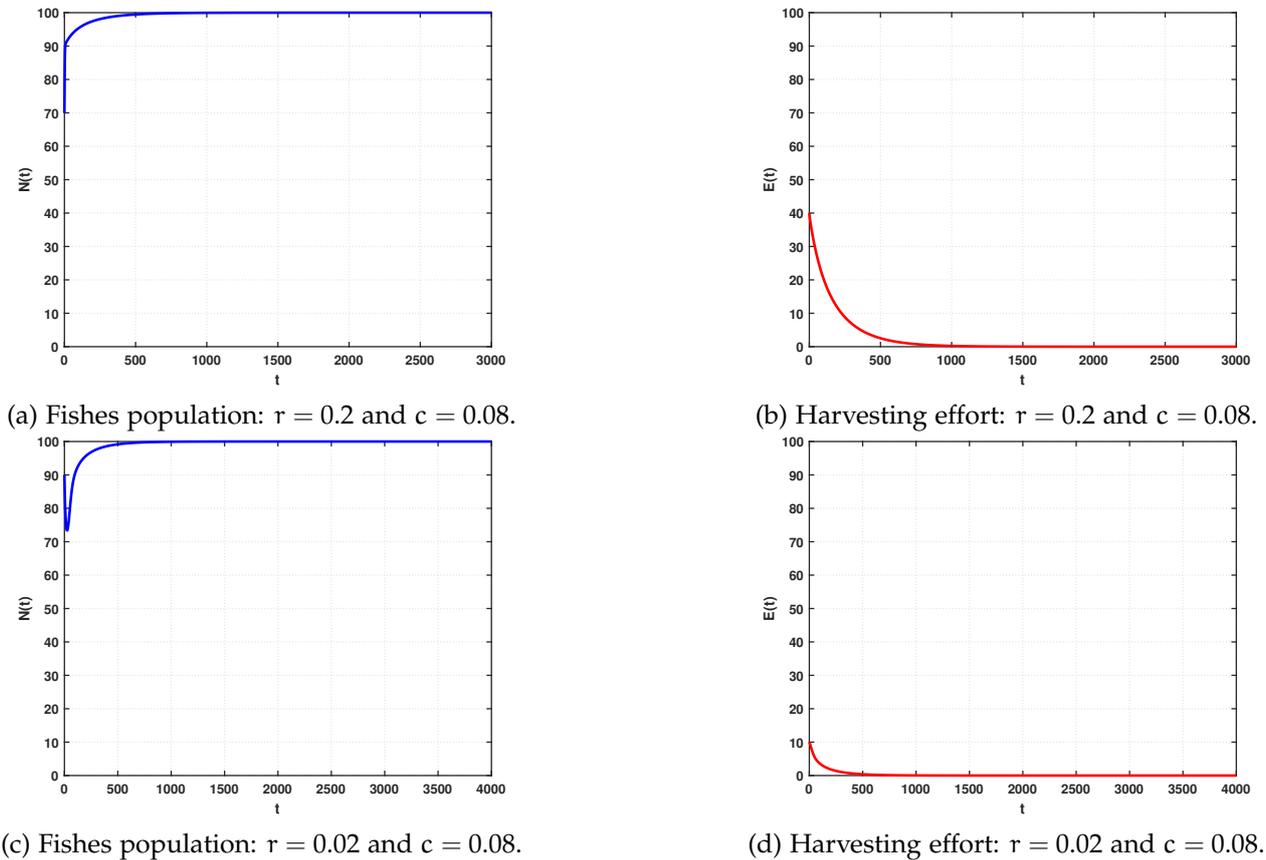
(d) Harvesting effort: $r = 0.02$ and $c = 0.08$.

Figure 6: Fishes population vs harvesting effort for $c = 0.08$.

As c passes $pqK/(\kappa + K) = 0.075$ to the value 0.08, β becomes bigger than the carrying capacity K and Equi(b_3) losses its stability, so the solutions tend to the equilibrium point Equi(b_2) $= (K, 0) = (100, 0)$. This scenario is illustrated in Figures 6a, 6b, 6c, and 6d.

5. Discussions and conclusions

This paper presented a harvesting model of fishes population, where the dynamics of fishes in absence of harvesting effort is governed by a logistic model with Allee effect, whereas the harvesting term is represented by a Holling functional response of type II. The proposed model has four equilibrium points Equi(b_0) $= (0, 0)$, Equi(b_1) $= (M, 0)$, Equi(b_2) $= (K, 0)$, and Equi(b_3) $= (\beta, p\beta(\beta - M)(K - \beta)/(cKM))$, where the local stability of each equilibrium point is analyzed and discussed. An explicit fitted numerical method is designed for solving the model. This numerical method is much faster than the Matlabs' solvers ode23 and ode45, and through it we generated the bifurcation diagrams that appeared in Figures 2a-2d by solving the model 10^5 times in 68.66 seconds, with average of 0.00069 seconds per one problem. The Matlab's solver ode45, solves the model at average time of 0.111505 seconds.

We found that for every value of $\kappa > 0$, there are points $c_{\delta_1}, c_\sigma^*, c_2^*$, and c_{δ_2}, such that $c_{\delta_1} < c_\sigma^* < c_2^* < c_{\delta_2}$. These values of c are such that $\delta = \det(J_3^*) = 0$ when $c = c_{\delta_1}$ or $c = c_{\delta_2}$, $\sigma = \text{trace}(J_3^*) = 0$ when $c = c_\sigma^*$ and $D = \sigma^2 - 4\delta = 0$ when $c = c_2^*$. The curves that show the relationships between κ, $c_{\delta_1}, c_\sigma^*, c_2^*$, and c_{δ_2} are illustrated in Figures 1b and 1a.

We considered several values of the parameter c for the numerical simulations that are aimed to confirm the theoretical results. The first case was when $c < c_\sigma^*$, where $\text{Equi}(b_0)$ is the only stable node. It showed that in the long term, the dynamics of the fishes population and effort tend to $\text{Equi}(b_0) = (0,0)$ (see Figures 3a, 3b, 3c, and 3d). The second case was when $c \approx c_\sigma^*$ (Figures 4b, 4b, 5a, and 5b), which shows oscillatory behaviour around $\text{Equi}(b_3)$, because the eigenvalues of J_3^* are almost pure imaginary. The third case was when $c_\sigma^* < c < c_2^*$, (where the eigenvalues J_3^* are complex with negative real parts), which showed that the solutions oscillate around $\text{Equi}(b_3)$ but converge it (Figures 4c, 4d, 5c, 5d, 4e, 4f, 5e, and 5f). The fourth case was when $c_\sigma^* < c < c_2^*$ (where the eigenvalues of J_3^* are real and negative), which showed convergence to $\text{Equi}(b_3)$ in the long term without oscillations (Figures 4g, 4h, 5g, and 5f). The last case is when $c > pqK/(\kappa + K)$, where N_3^* becomes greater than the carrying capacity K and the solution tend in the long term to the equilibrium point $\text{Equi}(b_2) = (K,0)$ (as appear in Figures 6a, 6b, 6c, and 6d).

The results obtained by the numerical simulations agree with and confirm the theoretical results obtained in Section 3.

References

[1] N. D. Barlow, *Harvesting models for resource-limited populations*, New Zealand journal of ecology, **10** (1987), 129–133. 1

[2] E. B. M. Bashier, K. C. Patidar, *Fitted numerical methods for a system of first order delay differential equations*, Proceedings of Neural, Parallel, and Scientific Computations (Atlanta, GA), **2010** (2010), 48–53. 4

[3] E. B. M. Bashier, K. C. Patidar, *A Comparison of Numerical Methods for Systems of First Order Delay Differential Equations Arising in Biology*, In: A Treatise of Biological Models, **2012** (2012), 75–96. 4

[4] K. L. Cooke, H. E. Nusse, *Analysis of the complicated dynamics of some harvesting models*, J. Math. Biol. **25** (1987), 521–542. 1

[5] A. Daci, *Fish Harvesting Models And Their Applications in a reservoir in Saranda, Albania*, J. Multidisciplin. Eng. Sci. Tech. (JMEST), **3** (2016), 5279–5282. 1

[6] A. Daci, A. Spaho, *Bifurcation in a dynamical system: harvesting models*, International Conference on Research and Engineering-Challenges Toward the Future (Albania), **2013** (2013), 24–25. 1

[7] R. P. Dunn, K. A. Hovel, *Predator type influences the frequency of functional responses to prey in marine habitat*, Biol. Lett., **16** (2019), 8 pages. 1

[8] E. González-Olivares, J. Mena-Lorca, A. Rojas-Palma, J. D. Flores, *Dynamical complexities in the Leslie-Gower predator–prey model as consequences of the Allee effect on prey*, Appl. Math. Model., **35** (2011), 366–381. 1

[9] M. W. Hirsch, S. Smale, R. L. Devaney, *Differential Equations, Dynamical Systems, and an Introduction to Chaos*, Third ed., Elsevier/Academic Press, Amsterdam, (2013). 1

[10] L. R. Huang, D. H. Cai, W. Y. Liu, *Optimal harvesting of an abstract population model with interval biological parameters*, Adv. Difference Equ., **2020** (2020), 17 pages. 1

[11] L. V. Idels, M. Wang, *Harvesting fisheries management strategies with modified effort function*, Int. J. Model. Iden. Control (IJMIC), **3** (2008), 83–87. 1

[12] M. Kot, *Elements of mathematical ecology*, Cambridge University Press, Cambridge, (2001). 1

[13] E. V. Leeuwen, V. A. A. Jansen, P. W. Bright, *How population dynamics shape the functional response in one-predator-two-prey system*, Ecology, **88** (2007), 1571–1581. 1

[14] L. Perko, *Differential equations and dynamical systems*, Springer-Verlag, New York, (2001). 3.2

[15] T. Pradhan, K. S. Chaudhuri, *Bioeconomic modelling of a single species fishery with Gompertz law of growth*, J. Biol. Syst., **6** (1998), 393–409. 1

[16] L. A. Real, *The Kinetics of Functional Response*, Amer. Natural., **111** (1977), 289–300. 1

[17] A. Rojas-Palma, E. González-Olivares, *Optimal harvesting in a predator-prey model with Allee effect and sigmoid functional response*, Appl. Math. Model., **36** (2012), 1864–1874 1

[18] A. Rojas-Palma, E. González-Olivares, B. González-Yañez, *Metastability in a Gause type predator–prey models with sigmoid functional response and multiplicative Allee effect on prey*, Proceedings of International Symposium on Mathematical and Computational Biology, **2007** (2007), 295–321. 1